Effect of Additives and Protective Coating on the Indirect Tensile Strength and Oblique Shear of Concrete under the Sulfate Attack and Salt Crystallization Using Hybrid FMEA and Fuzzy TOPSIS Technique

Fereydoun Abolghasemzadeh[1], Morteza Rayati Damavandi[2*], Maedeh Sadeghpour-Haji[3]

1- PhD student .Department of Civil Engineering, Faculty of Technical Engineering, Sari Branch, Islamic Azad University, Sari, Iran; +98 9113115133
2- *(Corresponding author) Assistant Professor, Department of Civil Engineering, Islamic Azad University, Ghaemshahr Branch, Iran; +989112142648,
3- Assistant Professor, Department of Civil Engineering, Islamic Azad University, Ghaemshahr Branch, Iran; +98 9112142648

Abstract

The fuzzy FMEA technique was used to identify failure risks in the operation of wastewater plants. The mentioned risks were found by employing experts in the water and sewage industry then a matrix of fuzzy RPN parameters was shaped, and the risks were ranked based on the fuzzy TOPSIS method. The results indicated that the risk of low durability of structural concrete (0.72) obtained the first rank of the cause leading to wastewater plant failure followed by the quality of inlet sewage (0.66) and appropriate repair and maintenance (0.63), which obtained second and third ranks, respectively. Because the quality of concrete structures exposed to wastewater was at first rank, it was decided on manufacturing resistant concrete in the laboratory. The concrete structures are obviously in contact with wastewater exposed to sulfate ions. These aggressive ions produce new compounds by reacting to hydration products causing a crack or splitting in the concrete due to expansion. Therefore, concrete protection solutions must be created in such environments. Additives and protective coatings are some of these solutions. The present study evaluated the effect of additives, including polymer latex and micro-silica, and protective coatings such as epoxy and crystallization on concrete durability under the simultaneous effect of sulfate attack and salt crystallization. For this purpose, concrete specimens were exposed to sodium sulfate solution and successive wetting-drying cycles. The decline in concrete strength resulting from destructive factors was then determined, by using indirect tensile strength and oblique shear strength tests. The results showed that a minimum reduction in indirect tensile strength occurs when using 10% latex and 5% micro-silica, while 20% latex and 10% micro-silica are used in the oblique shear test to achieve the minimum decline in this indirect tensile strength of concrete. Epoxy coating outperformed crystallization in case of increasing concrete durability.

Keywords: FMEA. TOPSIS, Sulfate Attack, Salt Crystallization, Indirect Tensile Strength, Oblique Shear Strength

Tob Regul Sci.™ 2022;8(2): 65-87
DOI: Doi.Org/10.18001/TRS.8.2.05

Introduction

A) Decision-making

1. Introduction

Municipal wastewater plants are mainly constructed to relatively improve the quality of wastewater collected from population centers and some industries where their sewage is mixed with municipal wastewater. The quality of treated wastewater prepared for disposal or reused in agriculture is determined based on the regulations associated with the environmental status of receptive waters and rules of sustainable development. The establishment of wastewater plants usually requires considerable investment and operation costs. Hence, proper operation and maintenance of these plants require specific importance in return on the considered investment. The wastewater plants are maintained and operated to keep their installations and equipment safe and pave the way for optimum operation and national investment.

Now, repair and maintenance systems play a vital role in the process of manufacturing, repair, and maintenance of considered devices and equipment under standard conditions. One can divide repair and maintenance actions into two preventive and corrective maintenance categories. Preventive maintenance tends to keep the structure and relevant equipment under suitable operational conditions by planning periodic visits and regular repairs. In contrast, corrective maintenance tends to repair and relaunch out-of-service and failed equipment and structure. Therefore, preventive structure and equipment are more important than the corrective ones because the first one prevents the treatment process failure imposing lower cost.

Repair and maintenance are one of the main pillars of every dynamic organization, which employs professional and productive experts and human forces to prevent failure in different units. The maintenance system directly affects the organization's funds and profit, while a lack of accurate planning for repair and maintenance decreases the equipment's lifetime. Reliability-based maintenance can create a logical interaction between repairmen, operators, managers, engineers, and all practitioners involved in the production of high-quality products. Reliability-based maintenance is the biggest change in the world of repair and maintenance. The reliability-based maintenance system is a prerequisite for the improvement of maintenance plans' effectiveness. Hence, organizations are highly interested in this approach.

The Brain Storming method and experts in the water and sewage industry were used to identify risks of failure in operating wastewater plants. Finally, 10 risks and options were suggested:

1. Ineffective management
2. Inappropriate equipment
3. Low durability of concrete structures

4. Poor financing
5. Improper operation
6. Quality and type of wastewater inlet
7. Unproductive manpower
8. Legal constraints
9. Improper organizational strategy
10. Inappropriate maintenance

The abovementioned risks were analyzed based on the FMEA[1] technique and criteria of risk occurrence, severity, and detection, and then were prioritized by using the Fuzzy TOPSIS model [1].

2. Decision tree model

The hierarchical analysis graph of multi-criteria decision-making methods [4] is usually determined at three levels objective, criteria, and options. Figure 1 depicts the hierarchy analysis graph of the present study.

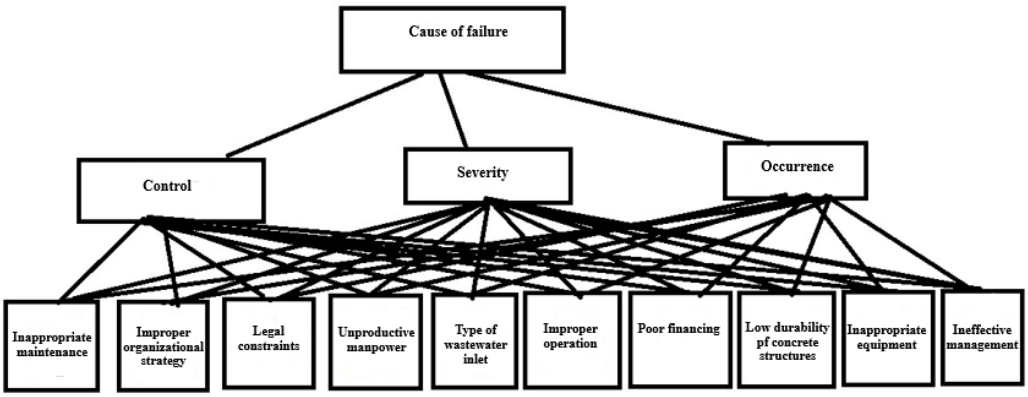

Figure 1. Hierarchy graph

3. Research and analysis phases in the decision-making process

3.1. Introducing FMEA technique

The FMEA method appeared in 1950 due to the importance of safety issues and preventing predictable incidences in the aerospace industry. In 1992, the SAE-J-1739 standard was introduced as an FMEA reference in the automotive industry. This technique became popular in recent years after the establishment of a quality assurance system in the automotive industry and published international QS 900 and IAFT 16949 standards [3].

FMEA is widely used to identify and eliminate the detected or potential failures of a system, design, and process. FMEA is an analytical technique that relies on "pre-occurrence prevention" to identify potential failure factors. This technique is a dynamic tool used to predict problems, defects, and

[1] Failure Mode and Effects Analysis

risks occurring during the design, development, and implementation of processes and services of the organization. FMEA is also used in the permanent improvement cycle. This study considers three important factors of the FMEA approach to rank the risks of the product [2]:

- Occurrence
- Severity
- Detection

1. Occurrence: it indicates the probability of failures' number relative to the number of processes;
2. Risk severity: it is the evaluation and assessment of a failure's result (if it occurs). Severity is an evaluation scale that defines the seriousness of the effect of a failure if occurs.
3. Detection: it indicates the probability of a failure detection before its occurrence effect is determined. The value or rank of detection depends on the control flow. Detection is the control ability to find the cause and mechanism of failures.

In traditional FMEA, risk factors (O-S-D) are simply multiplied by each other to find the risk priority number without considering the subjectivity and ambiguity in decision-makers' judgments. Moreover, the weight of risk factors (O-S-D) has also been eliminated. An FMEA approach has been proposed to overcome this problem and obtain a more logical rank for failure modes. Experts use linguistic variables to score and determine the D, O, and S of the FMEA model through fuzzy space [7].

Table 1. Verbal terms and their corresponding fuzzy numbers for options

Verbal variables for options	
Very poor (VP)	(1,0,0)
Poor (P)	(0,1,3)
Moderately poor (MP)	(1,3,5)
Moderate (M)	(3,5,7)
Moderately good (MG)	(5,7,9)
Good (G)	(7,9,10)
Very good (VG)	(9,10,10)

Table 2. Verbal terms and their corresponding fuzzy numbers for criteria

Verbal variables for options	
Very low (VL)	(0,0.05,0.1)
Low (L)	(0.05,0.1,0.2)
Moderately low (ML)	(0.2,0.3,0.4)
Moderate (M)	(0.3,0.4,0.5)
Moderately high (MH)	(0.5,0.6,0.7)
High (H)	(0.7,0.8,0.9)
Very high (VH)	(0.9,1,1)

After the hierarchies of the proposed model were created, comments of experts, including project managers were collected through a fuzzy questionnaire using linguistic variables.

Table 3 reports the experts' comments on three criteria of occurrence, severity, and control or detection using linguistic variables. Moreover, Table 4 presents the comments of experts about the occurrence, severity, and detection by using corresponding triangular fuzzy numbers.

Table 3. Experts' comments on the criteria using linguistic variable

			D1	D2	D3
	Occurrence	C1	H	VH	H
	Severity	C2	MH	H	H
	Detection	C3	ML	L	VL

Table 4. Experts' comments on the criteria using triangular fuzzy numbers

		D1			D2			D3		
Occurrence	C1	0.70	0.90	1.00	0.90	1.00	1.00	0.70	0.90	1.00
Severity	C2	0.50	0.70	0.90	0.70	0.90	1.00	0.70	0.90	1.00
Detection	C3	0.10	0.30	0.50	0.00	0.10	0.30	0.00	0.00	0.10

3.2. Introducing the Fuzzy TOPSIS[2] method

Multi-criteria decision-making techniques are subsets of research in operations, which have been developed based on mathematical and computational tools. TOPSIS technique is one of the multi-criteria decision-making methods used to rank a finite set of alternatives by Hwang and Yoon (1981). TOPSIS technique tries to select those alternatives with the shortest distance from the positive ideal and the furthest distance from the negative ideal solution. TOPSIS ranks the alternatives based on available information [5].

The fuzzy theory was introduced by Lotfi Askarzadeh known as Zadeh (1965) to model uncertainty in data existing in problems related to different sciences. Fuzzy techniques are preferred to classic and definite techniques for cases with inadequate data with ambiguity or uncertainty. The fuzzy TOPSIS technique was introduced by Chen (2000) to solve multi-criteria decision-making problems under uncertain conditions. TOPSIS method has been used in fuzzy logic of conducted previous studies. Linguistic variables have been used in the development process of the Fuzzy TOPIS technique to rank options and weight of criteria [6] because the application of lingual variables instead of numerical evaluation is more tangible and real when addressing unclassified and vague information, especially in modeling human judgments. This study used lingual variables and a direct weighing method to evaluate the importance of the criteria's weights and rank options. Tables 1 and 2 report the lingual variables and their corresponding triangular fuzzy numbers used by decision makers (D=1,2,…, K) to weigh options based on the fuzzy triangular numbers introduced by Chen (2000).

[2] Technique for Order Preference by Similarity to Ideal

3.2.1. Fuzzy TOPSIS phases (Chen, 2000)

Assume that the decision group consists of K members, the sum of criteria's weight and option ranking is done based on equations 1 and 2, where $\tilde{W}_j$ represents the weight of criterion j.

$$\tilde{W}_j = \frac{1}{K}\left[\tilde{W}_J^1 + \tilde{W}_J^2, ..., \tilde{W}_j^k\right] \quad (1)$$

$$\tilde{x}_{ij} = \frac{1}{k}\left[\tilde{x}_{ij}^1 + \tilde{x}_{ij}^2 + ... + \tilde{x}_{ij}^k\right] \quad (2)$$

According to this Matrix (D), $\tilde{x}_{ij}$ indicates the rank of option i (i=1,2,…,m) regarding the criterion j (j=1,2,…,n), which is based on lingual variables (Equation 3).

$$\tilde{x}_{ij} = (a_{ij}, b_{ij}, c_{ij}) \quad (3)$$

Stage 1: Creating a decision-making matrix of criteria and options

Equation 4 shows the decision-making matrix of criteria and options:

$$\tilde{D} = \begin{bmatrix} \tilde{x}_{11} & \tilde{x}_{12} & . & . & . & \tilde{x}_{1n} \\ \tilde{x}_{21} & \tilde{x}_{22} & . & . & . & \tilde{x}_{2n} \\ . & . & . & . & . & . \\ . & . & . & . & . & . \\ . & . & . & . & . & . \\ \tilde{x}_{m1} & \tilde{x}_{m2} & . & . & . & \tilde{x}_{mn} \end{bmatrix} \quad (4)$$

Table 5. Ranking options

			D1	D2	D3		D1	D2	D3		D1	D2	D3
Ineffective management	A	Occurrence	ML	MH	M	Severity	ML	M	ML	Detection	L	ML	VL
Inappropriate equipment	B		ML	M	MH		MH	M	MH		VL	VL	L
Low durability of concrete structures	C		VH	H	VH		VH	VH	H		M	MH	MH
Poor financing	D		M	MH	H		ML	M	ML		MH	M	ML
Improper operation	E		H	H	MH		M	MH	M		ML	L	ML
Quality and type of wastewater inlet	F		H	MH	MH		H	VH	VH		MH	H	MH
Unproductive manpower	G		ML	M	ML		ML	M	MH		M	ML	MH

Legal constraints	H		VL	L	VL		L	L	VL		L	VL	L
Improper organizational strategy	I		L	L	ML		M	ML	L		L	ML	VL
Inappropriate maintenance	j		H	MH	H		H	H	H		VL	L	ML

(5) $\tilde{W} = \left[\tilde{W}_1, \tilde{W}_2, ..., \tilde{W}_n\right]$

Stage 2: the fuzzy decision matrix must then become a comparable scale and normalized. Several methods are used for normalization. This study suggests several linear normalization methods. Now, lingual variables are converted to triangular fuzzy numbers. Table 6 reports the triangular fuzzy numbers to create a fuzzy decision-making matrix and fuzzy weight of each criterion.

Table 6. Fuzzy decision-making matrix

	Occurrence				Severity				Detection		
A	0.30	0.50	0.70		0.17	0.37	0.57		0.07	0.20	0.37
B	0.30	0.50	0.70		0.43	0.63	0.83		0.03	0.10	0.23
C	0.83	0.97	1.00		0.83	0.97	1.00		0.43	0.63	0.83
D	0.50	0.70	0.87		0.17	0.37	0.57		0.30	0.50	0.70
E	0.63	0.83	0.97		0.37	0.57	0.77		0.10	0.30	0.50
F	0.57	0.77	0.93		0.83	0.97	1.00		0.57	0.77	0.93
G	0.17	0.37	0.57		0.30	0.50	0.70		0.30	0.50	0.70
H	0.03	0.10	0.23		0.07	0.20	0.37		0.07	0.20	0.37
I	0.10	0.30	0.50		0.17	0.37	0.57		0.07	0.20	0.37
j	0.63	0.83	0.97		0.70	0.90	1.00		0.07	0.20	0.37
Weight	0.77	0.93	1.00		0.63	0.83	0.97		0.03	0.13	0.30

Stage 3: calculating normal fuzzy weighted matrix

The fuzzy decision matrix must be converted to a comparable scale and normalized in the next step. Several methods are used for normalization. This study suggests several linear normalization methods. In this lieu, equations 6-7 are introduced to normalize profit and cost criteria.

(6) $\tilde{R} = \left[\tilde{r}_{ij}\right]_{m \times n}$

(7) $$\tilde{r}_{ij} = \begin{cases} \left(\frac{a_{ij}}{c_j^*}, \frac{b_{ij}}{c_j^*}, \frac{c_{ij}}{c_j^*}\right), & j \in B \quad , c_j^* = \max c_{ij} \text{ if } j \in B \\ \left(\frac{a_j^-}{c_{ij}}, \frac{a_j^-}{b_{ij}}, \frac{a_j^-}{a_{ij}}\right), & j \in C \quad , a_j^- = \min a_{ij} \text{ if } i \in c \end{cases}$$

The normal decision-making matrix is normalized in this step as reported in Table 7.

Table 7. Normal decision-making matrix

	Occurrence				Severity				Detection		
A	0.30	0.50	0.70		0.17	0.37	0.57		0.07	0.21	0.39
B	0.30	0.50	0.70		0.43	0.63	0.83		0.04	0.11	0.25
C	0.83	0.97	1.00		0.83	0.97	1.00		0.46	0.68	0.89
D	0.50	0.70	0.87		0.17	0.37	0.57		0.32	0.54	0.75
E	0.63	0.83	0.97		0.37	0.57	0.77		0.11	0.32	0.54
F	0.57	0.77	0.93		0.83	0.97	1.00		0.61	0.82	1.00
G	0.17	0.37	0.57		0.30	0.50	0.70		0.32	0.54	0.75
H	0.03	0.10	0.23		0.07	0.20	0.37		0.07	0.21	0.39
I	0.10	0.30	0.50		0.17	0.37	0.57		0.07	0.21	0.39
j	0.63	0.83	0.97		0.70	0.90	1.00		0.07	0.21	0.39
Weight	0.77	0.93	1.00		0.63	0.83	0.97		0.03	0.13	0.30

Now, equation (8) is used to obtain a fuzzy weighted normal matrix.

(8) $\tilde{V} = [\tilde{v}_{ij}]_{m\times n}, \quad i = 1,2,...,m, \quad j = 1,2,....,n$

$\tilde{v}_{ij} = \tilde{r}_{ij} . \tilde{w}_j$ اگر

After normalization, the weighted normal matrix- that is obtained from the normal fuzzy matrix multiplied by the weight of criteria- is measured. Table 8 reports the results of this calculation.

Stage 4: positive ideal solution (FPIS, A^+) and negative ideal solution (FNIS, A^-) are measured based on the equations (9) and (10).

(9)

$$A^* = (\tilde{v}_1^*, \tilde{v}_2^*, ..., \tilde{v}_n^*)$$

(10)

$$A^- = (\tilde{v}_1^-, \tilde{v}_2^-, ..., \tilde{v}_n^-)$$

where $\tilde{v}_j^-$ = (0,0,0) and $\tilde{v}_j^*$ = (1,1,1).

Table 8. Normal weighted matrix

	Occurrence				Severity				Detection		
A	0.23	0.47	0.70		0.11	0.31	0.55		0.00	0.03	0.12
B	0.23	0.47	0.70		0.27	0.53	0.81		0.00	0.01	0.08
C	0.64	0.90	1.00		0.53	0.81	0.97		0.02	0.09	0.27
D	0.38	0.65	0.87		0.11	0.31	0.55		0.01	0.07	0.23
E	0.49	0.78	0.97		0.23	0.47	0.74		0.00	0.04	0.16
F	0.43	0.72	0.93		0.53	0.81	0.97		0.02	0.11	0.30
G	0.13	0.34	0.57		0.19	0.42	0.68		0.01	0.07	0.23
H	0.03	0.09	0.23		0.04	0.17	0.35		0.00	0.03	0.12
I	0.08	0.28	0.50		0.11	0.31	0.55		0.00	0.03	0.12
j	0.49	0.78	0.97		0.44	0.75	0.97		0.00	0.03	0.12
FPIS	1.00	1.00	1.00		0.97	0.97	0.97		0.30	0.30	0.30

FNIS	0.03	0.03	0.03		0.04	0.04	0.04		0.00	0.00	0.00

Stage 5: the distance of option i or positive (A^+) and negative (A^-) ideals was measured based on equations (11) and (12), while the distance between two triangular fuzzy numbers is calculated based on equation (2).

$$d_i^* = \left\{ \sum_{j=1}^{n} d\left(\tilde{v}_{ij}, \tilde{v}_j^*\right) \right\} \quad i = 1,2,..., m,\ j = 1,2,..., n \qquad (11)$$

$$d_i^- = \left\{ \sum_{j=1}^{n} d\left(\tilde{v}_{ij}, \tilde{v}_j^-\right) \right\} \quad i = 1,2,..., m,\ j = 1,2,..., n \qquad (12)$$

Numerical values of positive and negative ideals were measured based on the weighted fuzzy decision-making matrix. Finally, the comparative closeness of each option to the ideal solution and the weight of each option were determined and sorted as reported in Table 9.

Table 9. Weight of each option

	d+	d-	cc
A	1.49489	0.88034	0.37
B	1.32186	1.06254	0.45
C	0.69077	1.74486	0.72
D	1.30467	1.10687	0.46
E	1.09202	1.32605	0.55
F	0.83284	1.62998	0.66
G	1.47015	0.93610	0.39
H	1.93143	0.38942	0.17
I	1.66211	0.71254	0.30
j	0.90636	1.52472	0.63

Stage 6: now, the comparative closeness coefficient (CC_i) of option i is calculated based on equation (13):

$$CC_i = \frac{d_i^-}{\left(d_i^* + d_i^-\right)}, \quad i = 1,2,..., m \quad 0 \le cl_{i+} < 1 \qquad (13)$$ $i = 1,2,..., m$,

Options are ranked in descending order based on their CC_i. The best option is the closest option to the FPIS and the farthest option from FNIS. In other words, the higher the CC, the more ideal the corresponding option will be.

Finally, Table 10 reports the optional ranking considering the risk leading to the failure of wastewater plants.

Table 10. Ranking options

Low durability of concrete structures	C	CC3	0.72
Quality and type of wastewater inlet	F	CC6	0.66
Inappropriate maintenance	j	CC10	0.63

Improper operation	E	CC5	0.55
Poor financing	D	CC4	0.46
Inappropriate equipment	B	CC2	0.45
Unproductive manpower	G	CC7	0.39
Ineffective management	A	CC1	0.37
Improper organizational strategy	I	CC9	0.30
Legal constraints	H	CC8	0.17

4. Conclusion of the decision-making process

The results indicated that the proposed model was suitable for real-world problems under ambiguity and uncertainty. Moreover, findings reported the risk of low durability of concrete structure (0.72) at the first rank of cause leading to failure in the concrete structure of wastewater plants. This factor was followed by the type of wastewater inlet (0.66) and inappropriate maintenance (0.63) at the second and third ranks. Furthermore, improper operation (0.55), poor financing (0.46), inappropriate equipment (0.45), unproductive manpower (0.39), ineffective management (0.37), improper organizational strategy (0.30), and legal constraints (0.17) were in fourth to fifth ranks, respectively. Because the quality of concrete structures exposed to wastewater was at first rank, it was decided on manufacturing resistant concrete in the laboratory. This process has been explained in section B.

B) Laboratory

5. Introduction

Sulfate attack to concrete mainly converts calcium hydroxide to calcium sulfate, converts aluminate phase to ettringite, and decomposes calcium silica hydrate, which finally leads to concrete collapse. Various regulations, including American Concrete Institute (ACI) [1] and European Standard [2] are used to prevent and restore this damage. However, many studies have been conducted on the development of technology and new materials to examine concrete behavior under aggressive conditions to solve this issue and reduce the costs of concrete structures maintenance and restoration. Moreover, various experiments, such as oblique, Brazilian, pull-off, and other kinds of shear to evaluate the mechanical strength of new materials. The general classification of relevant studies on the effect of sulfate on concrete durability includes chemical attack of sulfate salts, salt crystallization, and simultaneous occurrence of these phenomena. Some of these studies have been mentioned herein.

Haufe and Vollpracht [3] studied the effect of sulfate ions on the direct tensile strengths of mortar specimens prepared by different kinds of cement. The results indicated a direct relationship between lower strength and ettringite formation. The more the volume of formed ettringite, the lower the strength will be. Zou et al. [4] proposed a mathematical model to predict the penetration depth of sulfate in concrete regarding the ion concentration and temperature of the solution. They validated the model and found that increased temperature of solution intensified the effects of

sulfate attack on strength reduction. Li et al. (5) studied the effect of the curing duration of concrete specimens on the compressive strength against sulfate attack. Their results indicated that a reduction in curing time increases the scaling and spalling of the surface of concrete specimens.
Another type of attack of sulfate salts on the concrete is done physically. In this case, sulfate salts enter through the solution into the capillary holes in the concrete. When the concrete is under successive drying and wetting cycles then the compression created by intermittent salt crystallization leads to concrete destruction. Many studies have been conducted on suitable concrete coatings to prevent this destructive phenomenon. These studies have been mentioned herein. Suleiman et al. [6] examined the effect of commercial coatings (saline, epoxy, bitumen, and acrylic) on the durability of concrete exposed to physical sulfate attack. They put the concrete specimens saturated with sulfate salt alternately under two environmental conditions: 20°C temperature, 82% humidity, and 40°C temperature, 31% humidity. They assessed the mass loss and considered visual assessment then found epoxy as the best coating and acrylic as the worse coating in protecting concrete against sulfate salt crystallization. Sakr et al. [7] studied the effect of the water-binder ratio and type of coating on the concrete resistance against sulfate salt crystallization. The results showed that concretes with higher water-binder ratios, epoxy, and ethyl silicate coatings create the required strength against sulfate salt crystallization. Sakr et al. [8] carried out another study on the strength of nano-clay/saline on the durability of concrete exposed to salt crystallization attack. The results indicated the optimum value of the nano-clay application of 5%-10% of saline weight in the coating. Bassuoni and Sakr [9] examined the application of the nano-silicate coating to overcome the physical effects of sulfate salt on the concrete. The results showed that 25%-50% nano-silicate with hydrophobic coating leaves a considerable effect on reducing concrete scaling. Sakr and Bassuoni [10] examined the strength of methyl-methacrylate, nano-clay/saline, and nano-silicate/saline coatings against physical sulfate attack. Their results showed that the strength of nanocoatings depends on the water-binder ratio in the concrete, while methyl-methacrylate coating with any water-binder ratio provides a suitable strength against salt solutions' penetration into the concrete.
It is worth noting that simultaneous effects of physical and chemical attacks of sulfate salts may occur on the concrete. In many marine structures within the distance between two hot water, concrete is more exposed to damage rather than other parts of the structure. Some studies have addressed this phenomenon. Gong et al. [11] studied the creep of concrete under various dry-wet circulations in a sulfate solution and proposed a mathematical model to assess this case. They concluded that an increased concentration of sulfate solution could increase the creep of the concrete. Chen et al. [12] studied the nano-structure, mass loss, and strength of mortars with different water-cement ratios under successive drying-wetting cycles. They found that an increased water-cement ratio led to a considerable increase in concrete damage while gypsum and sodium sulfate salts are sedimented in concrete holes. Li et al. [13] studied the durability of concrete made of magnesium potassium phosphate during drying, wetting, and in sodium sulfate solution. They found that fly ash could increase concrete durability, while quartz-containing aggregates reduced

the durability of this type of concrete. GUP et al. [14] investigated the effect of dry-wet frequency on compressive strength, tensile strength, and dynamic module. They found that the highest concrete deterioration occurs in the cycle in which, the dry-wet ratio is 5:1. Li et al. [15] studied the chemical and mechanical effect of sulfate solution on high-ductility concrete. Their results showed that polyvinyl alcohol microfiber could help concrete keep its ductility after being damaged.

Finally, it should be noted that concretes damaged by the chemical and mechanical attack of sulfate salts require repair and maintenance operations. Moreover, many studies have evaluated the repaired concretes. Arianmanesh and Esfahani [16] investigated the effect of surface texture and curing conditions on bond strength in the oblique shear experiment. Their results indicated the considerable effect of these parameters on the composite specimen failure model. Shekarchi Zadeh et al. [17] studied the continuity resistance in the oblique shear experiment between usual and ultra-high-performance concrete. Their results indicated that concrete curing by using sandblasting more considerably increases continuity strength rather that brushing with a wire brush and grooving the concrete surface. Sadrmomtazi and Ghodousian [18] studied the indirect tensile strength between fiber-reinforced self-compacting concrete and ordinary concrete, by using pull-off, push-out, and prism tests. Their results showed that fiber application with compaction control caused by drying increases indirect tensile strength. Sadrmomtazi et al. [19] investigated the bonding strength between polymer and usual concretes using a pull-off test. They reported that the bond strength between polymer and usual concretes is less than the bond strength between polymer modified and usual strength. Mansour and Fayed [20] examined the effect of concrete surface roughness on the bond strength between reinforced and ordinary concretes. Their results indicated the significant effect of surface roughness on the bond strength so that epoxy sticks and grooves, and circular holes could increase bond strength in the oblique shear experiment.

The literature review indicated the importance of studies on concrete durability against an aggressive environment. It also indicates further studies must be done on tensile and shear strength between repair materials and old concrete under the simultaneous chemical and mechanical attack of sulfate salts. Therefore, this study aims to examine the durability of repair materials and restored concrete exposed to the chemical mechanical attack of sulfate salt. To do this, different types of commercial materials and coatings for concrete protection with micro-silica and polymer latex-containing concrete were used. The loss of indirect tensile strength and shear strength under the successive wetting-drying cycles in sodium sulfate solution was assessed to evaluate the concrete durability.

6. Materials and Method

According to studies conducted by researchers, sulfuric substances and their compounds in wastewater cause corrosion in concrete installations. If the oxygen soluble in water is reduced, anaerobic bacteria are activated in the sludge layer adjacent to the concrete walls. The anaerobic bacteria revive the sulfate existing in wastewater to sulfide, which is then combined with the

hydrogen ions in the wastewater and releases the hydrogen sulfide gas from the wastewater surface. Finally, hydrogen sulfide gas is oxidated to sulfuric acid y aerobic bacteria. When sulfuric acid contacts with cement paste, calcium hydroxide is firstly converted to gypsum based on equation (1).

$$Ca(OH)_2 + H_2SO_4 \rightarrow CaSO_4 + 2H_2O \quad (1)$$

The gypsum then reacts to calcium aluminum based on equation (2) and produces ettringite.

$$3CaSO_4.2H_2O + 3CaO.Al_2O_3 + 26H_2O \rightarrow (CaO)_3.(Al_2O_3).(CaSO_4)_3.32H_2O \quad (2)$$

Chemical reactions in equations (1) and (2) indicate that the biological corrosion of concrete is a compound acid-sulfate process [21]. This reaction produces gypsum and ettringite that do not have structural strength and adhesive properties, and their volume is 2-7 times greater than the raw ingredients of cement paste [22]. This expansion in volume creates a crack in the concrete increasing its permeability. This process is repeated through time and the deterioration of damaged layers, while concrete underlayers are exposed to sulfate ions and fully deteriorated. This mechanism destroys concrete facilities and imposes heavy repair costs worldwide. For instance, concrete corrosion in concrete pipes for sewage transfer has caused a 500 million dollars of loss for the sewage collecting network in Los Angles [23]. Therefore, proper coating and repair materials extend the operation lifetime of sewage concrete facilities and reduce the cost of repair and maintenance. In line with this necessity, the present paper examines the behavior of repair materials and coatings that protect concrete in a sulfate environment.

6.1. Materials

The consumable materials included fine-grained mineral stones with a specific density of 2.67 and a water absorption rate of 1.3% following ASTM C128 Standard. Following the ASRM C127 standard, coarse-grained stones were used with a maximum mineral aggregate size of 12.5mm with a specific density of 2.71 and a water absorption rate of 1%. Stone materials were granulated based on the ASTM C33 Standard. Type II cement was used based on the ASTM C150 Standard, and micro-silica powder was selected based on the ASTM C1240 standard. The F-type super-lubricant additive based on the polycarboxylate ether was used following ASTM C494 Standard to prevent reduction in efficiency of micro-silica-containing mixtures. The latex-based additive was used to manufacture the modified polymer concrete. Moreover, three types of repair materials and two commercial anti-corrosion coatings were used. The repair materials of types (A), (B), and (C) included ready-to-use mortar without shrinkage with 7-day compressive strength of more than 40 MPa, so that Type (B) contained micro-fiber and Type (C) contained both micro-fiber and anti-sulfate cement. Anti-corrosion coating of Type (A) is crystallizing additive. This coating contains nonorganic compounds creating an integrated and non-permeable surface through deep

permeability in concrete and reaction to the available lime. Type (B) coating is a two-component modified epoxy-based coating.

6.2. Method

According to European Standard [2], concrete repair and strengthening against chemical and mechanical attack of sulfate salt is done respectively within two methods: reinforcing the concrete's materials and protecting the concrete surface against ingress. Hence, micro-silica, latex, and three types of commercial repair materials (A), (B), and (C) were used to reinforce the anti-corrosion properties of the concrete's ingredients. It is worth noting that micro-silica increases concrete durability by producing secondary silica calcium hydrates, and latex provides strength against splitting by increasing the tensile strength of cement paste [24]. Three mass rates of cement (5%, 10%, 15%) were used to examine the effect of micro-silica on the concrete resistance against sulfate attack. Moreover, three 10%, 20%, and 30% mass rates of cement were used to find the effect of polymer latex on the concrete resistance against sulfate attack. The indirect tensile and shear strengths were evaluated after observing the changes in concrete strength in presence of additives and comparing it with the concrete mixture without additives and commercial repair materials. Two types of coatings (crystallizable coating type A and epoxy type B) were used to make the concrete surface resistant to ingress. The strength of each coating against wetting-drying cycles was then examined. The simultaneous effect of micro-silica and polymer latex on preventing concrete strength loss against chemical attack and crystallization of sulfate salt was evaluated in the next step. Table 11 reports the design of considered mixtures.

Table 11. Repaired concrete mixture

Design Number	Gravel (kg/m3)	Sand (kg/m3)	Cement (kg/m3)	W/CM	SF/CM	Latex/CM	SP/C
Mixtures without protecting coatings							
1	1038	595	500	0.42	---	---	0.003
2	1038	595	450	0.42	---	0.1	---
3	1038	595	400	0.42	---	0.2	---
4	1038	595	350	0.42	---	0.3	---
5	1038	595	475	0.42	0.05	---	0.005
6	1038	595	450	0.42	0.10	---	0.005
7	1038	595	425	0.42	0.15	---	0.007
8	Ready-to-use commercial mortar without shrinkage and type (A) containing micro-fiber						
9	Ready-to-use commercial mortar without shrinkage and type (B)						
10	Ready-to-use commercial mortar without shrinkage and type (C) containing micro-fiber and anti-sulfate cement						
11	1038	595	500	0.42	---	---	0.003

12	1038	595	400	0.42	---	0.2	---
13	1038	595	450	0.42	0.10	---	0.005
14	1038	595	350	0.42	0.10	0.2	0.003
15	Ready-to-use commercial mortar without shrinkage and type (A) containing micro-fiber						
16	Ready-to-use commercial mortar without shrinkage and type (B)						
17	Ready-to-use commercial mortar without shrinkage and type (C) containing micro-fiber and anti-sulfate cement						

Resistance of additives and repair materials in a sulfate environment was evaluated using indirect bond tensile strength and oblique shear strength tests.

6.2.1. Construction of specimens and curing process

The concrete was produced based on the ASTM C192 Standard and a report published by American Concrete Institute ACI 458.3R [25]. Aggregates were used with saturated mode and dry surface. The materials were added to the mixer in a row: coarse-grained, fine-grained, powder materials, and water. First, coarse-grained materials and 70% water were poured into the mixer, and the device started working. The rest of the materials were added in the next step, and mixing operations continued for 3 minutes. Additives were separately mixed with the remaining water and added to the mixer. Finally, the mixing process was continued for 2 minutes, and concrete was poured into molds. According to Table 11, one semi-cylinder with a 15×30cm size and one 10×20cm semi-cylinder were prepared in each mixture design for oblique shear and indirect tensile strength tests, respectively. The plastic foam cut in the mold (as shown in Figure 2) was used to produce semi-cylinder specimens. Moreover, no oil was used on the oblique surface of the plastic foam cut not to weaken the bond between old concrete and repair materials. The repair operations on the base concretes were done based on the mixture design (1) reported in table 11. After concretes were poured into molds, their surfaces were protected using a suitable coating to prevent evaporation then the specimens were molded within 24 hours. Wet curing was done on all specimens for 28 hours in the next phase.

)B( )A(

Figure 2. (A) prepared plastic foam for oblique shear test, (B) base concrete for indirect tensile test

The surface of semi-cylinder specimens was then grooved, by using a wire brush based on the ICIR standard [26]. Semi-cylinder specimens were saturated again for 24 hours in the next step and put into the molds as shown in Figure 3. After the concrete's surface obtained sufficient moisture, the repair materials were put in the mold close to the initial concrete based on the all of mixture designs reported in Table 11.

)B( )A(

Figure 3. placing concrete semi-cylinder specimen to construct specimen (A) oblique shear test (B) indirect tensile test

After one day, the prepared specimen molds are opened to test their oblique shear and indirect tensile strengths, and moist curing was immediately redone for 28 hours. Finally, the selected specimens exited from the curing cycle and crystallizing and epoxy coatings were implemented on the concrete specimens' surface using a brush. It should be noted that coating (A) is implemented immediately after exiting specimens are taken out from the curing pond, while coating (B) is implemented on the specimen surface after the drying process.

6.2.2. Wetting-drying cycles

Pure 150gr sodium sulfate per liter of deionized water was used to create the simultaneous effect of sulfate attack and salt crystallization. Specimens were then immersed in the sodium sulfate solution for one week. The wetting-drying cycle was begun so that specimens were immersed in the sodium sulfate for 2 days, and then were dried at 110°C temperature for one day. This cycle was repeated 60 times for each specimen. The specimens were finally tested.

6.2.3. Conducted tests

An indirect tensile strength test was done by statistically loading on the side surface of 10×20cm semi-cylinder specimens based on the ASTM C496. The indirect tensile strength of concrete specimens is measured using Equation (1).

$$f_P = \frac{2F}{\pi D l} \quad (1)$$

where f_p, F, D, and l represent bond strength in a tensile mode based on megapascal (MPa), the applied force based on newton (N), the diameter of the specimen based on millimeter (mm), and the length of the specimen based on millimeter (mm).

the oblique shear test was done on 15×30cm cylinder specimens following ASTM C882 standard. The upper and lower surfaces of specimens were coated using neoprene based on the ASTM C1231Standard before being tested. The loading was applied on specimens within force control mode and statically by using a fully automatic hydraulic jack. The bond strength in the shear loading mode of concrete specimens is measured based on equation (2).

$$f_S = \frac{F \sin(2\alpha)}{2A} \quad (2)$$

In equation (2), f_s, F, A, and α indicate bond strength within shear loading mode based on megapascal (MPa), the applied force based on Newton (N), the section of the specimen based on the squared millimeter (mm^2), and angle of the diagonal surface of a specimen relative to the vertical axis.

7. Results and test analysis

7.1. Effect of additives and protective coating on indirect tensile strength of concrete exposed to sulfate attack and salt crystallization

Figures 3-5 depict the effect of latex, micro-silica, and protective coatings on the indirect tensile strength of concrete exposed to sulfate attack and salt crystallization. The concrete cylinder splitting test was used to determine bond strength under indirect tensile loading. According to Figure 4, an increase in latex value leads to a 20% increase in bond tensile strength. Moreover, the lowest loss occurred in the 10% specimen under the effect of the wetting-drying cycle. According to Figures 4 and 5, sulfate ion penetration into the concrete bond severely destroys the concrete bond strength reducing it up to one-third in the concrete that contains no additive. This test is highly important

for selecting repair materials because is a metric used to indirectly measure adhesion between old concrete beneath the structure and repair materials. According to Figure 5, a 10% increase in micro-silica leads to higher bond strength and then remains fixed. Various criteria have been provided to evaluate indirect tensile strength. According to Virginia Transportation Authority [27], the bond tensile strength greater than 2.1 MPA is perfect, 1.7-2.1 MPa is very good, 1.4-1.7 MPa is good, 0.7-1.4 MPa is medium, and <0.7 MPA is weak.

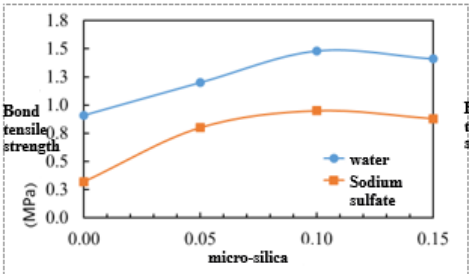

Figure 5. Changes in indirect tensile strength compared to variations (%) in micro-silica exposed to wetting-drying cycle

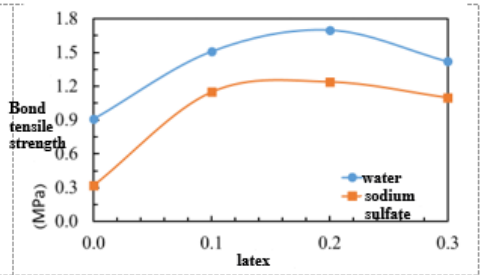

Figure 4. Changes in indirect tensile strength compared to variations (%) in latex exposed to wetting-drying cycle

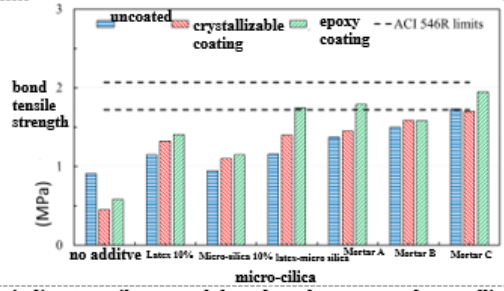

Figure 6. Changes in indirect tensile strength based on the epoxy and crystallizable coating exposed to wetting-drying cycle

Furthermore, American Concrete Institute ACI 546R [28] reports one-day, 7-day, and 28-day bond tensile strength equal to 0.5-1 MPA, 1-1.7 MPa, and 1.7-2.1 MPa. Figure 6 shows the effect of coating on the indirect tensile strength in comparison with the ACI 546R standard [28]. As is expected, the concrete without any additive has the highest indirect tensile strength against wetting-drying cycles, while protective coatings cannot singly prevent concrete damage. It is worth noting that protective coating could affect the indirect tensile strength of the concrete that contains no additive. The minor strength loss in concrete containing no additive shown in Figure 6 proves this case. Under wetting-drying cycles, mortar A with epoxy coating and mortar C have bond tensile strength criteria. Moreover, the results obtained from this study are matched with findings obtained by Geissert [29]. Regardless of the type of concrete mixture design, all specimens were raptured from the contact surface of initial and repaired concrete as shown in Figure 7. This is a predictable case because the bond strength between repair materials and old concrete is half of the indirect tensile strength of concrete repair materials in the best mode.

Figure 7. Rapture mode of repaired concrete specimen in an indirect tensile test

7.2. Effect of additives and protective coating on the oblique shear strength of concrete exposed to sulfate attack and salt crystallization

Figures 8-10 indicate the effect of latex, micro-silica, and protective coatings on the oblique shear strength of concrete exposed to sulfate attack and salt crystallization. in general, test results show that oblique shear strength is greater than the tensile strength. Silfwerbrand has also reported this case. The oblique shear test has been used to determine the bond strength under compressive and shear loading. This test has been approved by many standards [28 & 31]. Figures 8 and 9 indicate that sulfate attack reduces the oblique shear strength. Moreover, these figures show that although oblique shear strength is reduced or remained fixed after adding latex and micro-silica, these additives had positive durability effects preventing the severe strength loss caused by sulfate attack and salt crystallization. As shown in figure 8, a 20% increase in latex volume leads to a reduction in oblique shear strength then it becomes fixed. The reason is that the initial concrete is damaged due to the destructive effects of sulfate attack and salt crystallization, so an excessive increase in latex does not lead to a change in bond strength. According to Figure 9, a 5% increase in micro-silica leads to a decrease in oblique shear strength then remains unchanged due to the added micro-silica and rapture model control by the old concrete. In this case, the old concrete is damaged under the applied force and loading, so micro-silica variations do not affect the test result. In Figure 10, some oblique shear strengths do not satisfy the standard rates because the strength of old concrete is reduced, and then splitting occurs in it due to the wetting-drying cycle.

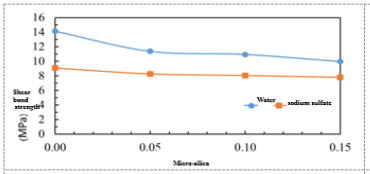

Figure 9. changes in oblique shear strength compared to variations (%) in micro-silica exposed to wetting-drying cycle

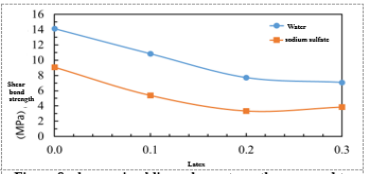

Figure 8. changes in oblique shear strength compared to variations (%) in latex exposed to wetting-drying cycle

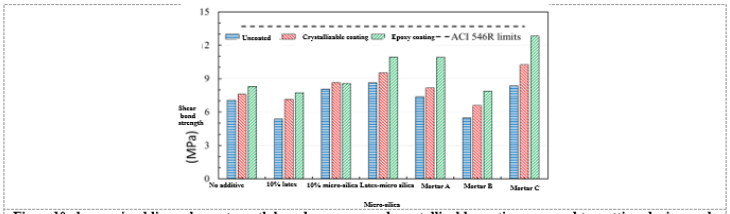

Figure10 changes in oblique shear strength based on epoxy and crystallizable coatings exposed to wetting-drying cycle

When micro-silica and latex are simultaneously added, the oblique shear strength of concrete will be increased. Figure 10 examined the effect of coating on the oblique shear strength and compared it with the ACI 546R standard [28]. The results indicated that mortars A and C with epoxy coating had the highest bond shear strength within the wetting-drying cycle.

Figure 12. Rapture in repair concrete

Figure 12. Rapture in the contact surface

Figure 11. Rapture in old concrete

Figures 11-13 depict the rapture modes. The rapture mode and bond strength provide useful information about the efficiency of repair materials. If rapture fully occurs on the contact surface, the real bond strength will be obtained. Rapture in other points indicates that bond strength is greater than the old and repair concrete strength. If the rapture occurs in the old concrete, the repair concrete is suitable/ rapture shape of each specimen was visually examined and classified as a failure mode in old concrete, contact surface, repair concrete, and composite concrete. Moreover, roughness in the contact surface has a considerable effect on the result of the oblique shear test [32 & 33]. The results are conservative because the old concrete surface has been grooved by a brush.

8. Conclusion

The present paper examined the effect of polymeric and pozzolan additives and protective coatings on the indirect tensile strength and oblique shear strength under the sulfate attack and salt crystallization. The following results were obtained:

A) Polymetric latex and micro-silica additives could reduce the indirect tensile strength loss caused by the wetting-drying cycle. In this case, latex polymer (10%) and micro-silica (5%) had the highest effect on preventing indirect tensile strength loss of concrete.

B) The micro-silica additive could decrease the oblique shear strength loss caused by the wetting-drying cycle. In this case, micro-silica (%) had the highest effect on preventing oblique shear strength loss of concrete.

C) Epoxy coating outperformed the crystallizable coating in the field of strength against the destructive effects of sulfate attack and salt crystallization.

References

1. [1] Habibi, H., Talebi, S., Khonakdar, M., Akbarpoor, S. (2013). Evaluating and prioritizing safety risks in operation process based on EMEA and TOPSIS models, 28th International Conference on Electricity, Issue F-13-AAA-0000
2. [2] Zadeh, L.A. 1996. Fuzzy sets. In Fuzzy Sets, Fuzzy Logic, And Fuzzy Systems: Selected Papers by Lotfi A Zadeh (pp. 394-432).
3. [3] Fattahi, R. & Khalilzadeh, M. 2018. Risk evaluation using a novel hybrid method based on FMEA extended MULTIMOORA and AHP methods under a fuzzy environment. Safety Science, 102, pp.290-300.
4. [4] Hwang, C.L. & Yoon, K. 1981. Methods for multiple attribute decision making. In Multiple attribute decision making (pp. 58-191). Springer, Berlin, Heidelberg.
5. [5] Chen, C.T. 2000. Extensions of the TOPSIS for group decision-making under fuzzy environment. Fuzzy sets and systems, 114(1), pp.1-9.
6. [6] Braglia, M., Frosolini, M., & Montanari, R. (2003). Fuzzy TOPSIS approach for failure mode, effects, and criticality analysis. Quality and Reliability Engineering International, 19,425–443.
7. [7] Chin, K. S., Chan, A., & Yang, J. B. (2008). Development of a fuzzy FMEA-based product design system. International Journal of Advanced Manufacturing Technology,
8. 36, 633–649.
9. ACI 562M-13. (2013). Code Requirements for Assessment, Repair, and Rehabilitation of Existing Concrete Structures and Commentary. Farmington Hills, MI, USA: American Concrete Institute.
10. British Standards Institution (BSI). (2003). BS EN 1504 Products and systems for the protection and repair of concrete structures. Definitions, requirements, quality control, and evaluation of conformity.
11. Haufe, J., & Vollpracht, A. (2019). Tensile strength of concrete exposed to sulfate attack. *Cement and Concrete Research*, *116*, 81-88.
12. Zou, D., Qin, S., Liu, T., & Jivkov, A. (2021). Experimental and numerical study of the effects of solution concentration and temperature on concrete under external sulfate attack. *Cement and Concrete Research*, *139*, 106284.
13. Li, X., Yu, X., Zhao, Y., Yu, X., Li, C., & Chen, D. (2022). Effect of initial curing period on the behavior of mortar under sulfate attack. *Construction and Building Materials*, *326*, 126852.
14. Suleiman, A. R., Soliman, A. M., & Nehdi, M. L. (2014). Effect of surface treatment on the durability of concrete exposed to physical sulfate attack. *Construction and Building Materials*, *73*, 674-681.
15. Sakr, M. R., Bassuoni, M. T., & Taha, M. R. (2019). Effect of coatings on concrete resistance to physical salt attack. *ACI Materials Journal*, *116*(6), 255-267.

16. Sakr, M. R., Bassuoni, M. T., & Ghazy, A. (2021). The durability of Concrete Superficially Treated with Nano-Silica and Silane/Nano-Clay Coatings. *Transportation Research Record*, *2675*(9), 21-31.
17. Sakr, M. R., & Bassuoni, M. T. (2021). Silane and methyl-methacrylate-based nanocomposites as coatings for concrete exposed to salt solutions and cyclic environments. *Cement and Concrete Composites*, *115*, 103841.
18. Liao, Y. D., Yang, Y. C., Jiang, C. H., Feng, X. G., & Chen, D. (2015). Degradation of mechanical properties of cementitious materials exposed to wet–dry cycles of sulfate solution. *Materials Research Innovations*, *19*(sup5), S5-173.
19. Gong, J., Cao, J., & Wang, Y. F. (2016). Effects of sulfate attack and dry-wet circulation on creep of fly-ash slag concrete. *Construction and Building Materials*, *125*, 12-20.
20. Chen, H., Huang, H., & Qian, C. (2018). Study on the deterioration process of cement-based materials under sulfate attack and drying–wetting cycles. *Structural Concrete*, *19*(4), 1225-1234.
21. Li, Y., Shi, T., Li, Y., Bai, W., & Lin, H. (2019). Damage of magnesium potassium phosphate cement under dry and wet cycles and sulfate attack. *Construction and Building Materials*, *210*, 111-117.
22. Guo, J. J., Wang, K., Guo, T., Yang, Z. Y., & Zhang, P. (2019). Effect of dry–wet ratio on properties of concrete under sulfate attack. *Materials*, *12*(17), 2755.
23. Li, L., Shi, J., & Kou, J. (2021). Experimental Study on Mechanical Properties of High-Ductility Concrete against Combined Sulfate Attack and Dry–Wet Cycles. *Materials*, *14*(14), 4035.
24. Arianmanesh, S., Esfahani, M. R. (2013). Investigation into compatibility between repair material and substrate concrete, Journal of Civil and Environmental Engineering, University of Tabriz, 43.1(70), 1-13.
25. Shekarchi Zadeh, M., Jafari Nejad, S., Rabiee, A.M. (2019). Experimental study of continuity resistance between usual and ultra-high-performance concrete, Journal of New Approaches in Civil Engineering, 3(3), 19-29.
26. Sadrmomtazi, A., Ghodousian, O. (2019). Comparison of pull-off, push-out, and splitting prism tests for assessment of bonding between fiber-reinforced self-compacting concrete as a repair layer and concrete substrate, Journal of Structural and Construction Engineering, 6(4), 199-212.
27. Sadrmomtazi, A., Kohani Khoshkbijari, R., Maleki Khoshkbijari, M., Amooie, M. (2020). An investigation on mechanical properties and bonding strength of polymer concretes and polymer modified concretes as repair overlays on the concrete substrate, Journal of Structural and Construction Engineering, 7(1), 41-55.
28. Mansour, W., & Fayed, S. (2021, February). Effect of interfacial surface preparation technique on bond characteristics of both NSC-UHPFRC and NSC-NSC composites. In *Structures* (Vol. 29, pp. 147-166). Elsevier.

29. Paing, J., Picot, B., Sambuco, J. P., & Rambaud, A. (2000). Sludge accumulation and methanogenic activity in an anaerobic lagoon. *Water science and technology*, *42*(10-11), 247-255.
30. Cao, H. T., Bucea, L., Ray, A., & Yozghatlian, S. (1997). The effect of cement composition and pH of the environment on sulfate resistance of Portland cement and blended cement. *Cement and Concrete Composites*, *19*(2), 161-171.
31. Sydney, R., Esfandi, E., & Surapaneni, S. (1996). Control concrete sewer corrosion via the crown spray process. *Water environment research*, *68*(3), 338-347.
32. Page, C. L., & Page, M. M. (Eds.). (2007). *The durability of concrete and cement composites*. Elsevier.
33. ACI Committee. (1995). State-of-the-art report on polymer-modified concrete. *American Concrete Institute, ACI*, *548*, Farmington Hills, MI.
34. ICRI (International Concrete Repair Institute). (2013). Selecting and specifying concrete surface preparation for sealers, coatings, polymer overlays, and concrete repair. *Guideline 310.2 R-2013*.
35. Sprinkel, M. M., & Ozyildirim, C. (2000). *Evaluation of high-performance concrete overlays placed on Route 60 over Lynnhaven Inlet in Virginia* (No. VTRC-01-R1). Virginia Transportation Research Council.
36. ACI Committee. (2006). Guide for the selection of materials for the repair of concrete. *American Concrete Institute*, *ACI 546R*, Farmington Hills, MI.
37. Geissert, D. G., Li, S. E., Franz, G. C., & Stephens, J. E. (1999). Splitting prism test method to evaluate concrete-to-concrete bond strength. *Materials Journal*, *96*(3), 359-366.
38. Silfwerbrand, J. (2003). Shear bond strength in repaired concrete structures. *Materials and Structures*, *36*(6), 419-424.
39. American Association of State Highway and Transportation Officials. (2010). Load and resistance factor design (AASHTO, LRFD). *Bridge design specifications. 5th ed.* Washington, DC.
40. Momayez, A., Ehsani, M. R., Ramezanianpour, A. A., & Rajaie, H. (2005). Comparison of methods for evaluating bond strength between concrete substrate and repair materials. *Cement and concrete research*, *35*(4), 748-757.
41. Wall, J. S., & Shrive, N. G. (1988). Factors affecting the bond between new and old concrete. *Materials Journal*, *85*(2), 117-125.